Supporting Information: Catalytic Mechanism of RNA Backbone Cleavage by Ribonuclease H from QM/MM Simulations

Edina Rosta[1], Marcin Nowotny[2], Wei Yang[3], Gerhard Hummer[1]*

[1]Laboratory of Chemical Physics, National Institute of Diabetes and Digestive and Kidney Diseases, National Institutes of Health, Bethesda, Maryland 20892-0520, U.S.A.

[2]Laboratory of Protein Structure, International Institute of Molecular and Cell Biology, 4 Ks. Trojdena Street, 02-109 Warsaw, Poland

[3]Laboratory of Molecular Biology, National Institute of Diabetes and Digestive and Kidney Diseases, National Institutes of Health, Bethesda, Maryland 20892, U.S.A.

Stability of Reactant State. We found that after equilibration and free energy sampling, the structure of the reactant state did not change significantly from the original X-ray crystal structure regardless of the protonation state of the Asp132.[1] The RMSD of the heavy atoms of the QM region was about 0.8 Å. The reactant structures show that Glu188 and the downstream phosphate help position the nucleophilic water molecule for an in-line, S_N2-type attack. The initial coordination of the ligands around the two Mg^{2+}-ions remains practically intact. The most significant change occurs for Glu188, which is coordinated at a somewhat closer distance to the metal ion than in the crystallographic structures (~2.1 Å *vs.* ~2.6 Å). During prolonged equilibration of the reactant state we also observed that this residue flips out of the active site, which is consistent with X-ray crystal structures.[1] NMR studies also found this loop to be flexible, albeit in the absence of substrate.[2]

In our simulations, the protonated Asp132 binds to metal ion B consistently in a monodentate fashion. In contrast, we find that unprotonated Asp132 fluctuates between monodentate and bidentate binding modes, as in earlier simulations.[4] The crystal structures show only monodentate binding, which would seem to imply that Asp132 is indeed protonated. However, we found that the average distance between metal ion B and the transiently interacting carboxylate oxygen (2.6 Å) is sufficiently close to the crystallographic value (2.8 Å in 1ZBL) that we cannot draw firm conclusions concerning the protonation state of Asp132 from the structure alone.

Protonation of Leaving Group via Ribose O2'. As a possible alternative to the protonation by Asp132, we explored a variant of pathway IIb in which a hydronium ion placed near the ribose O2' serves as the proton donor. In unbiased QM/MM dynamics simulations starting from the phosphorane intermediate with Asp132 unprotonated, we found that the proton readily transferred from the hydronium to the O2' oxygen, whose H2' proton then transferred transiently (for about 2.5 ps) to the carboxylate oxygen of Glu109 coordinated to metal ion B. From there, the proton reached the O3' leaving group, where it remained until the termination of the simulation (for about 5 ps). This rapid transfer from the hydronium to the leaving group suggests that there is no appreciable energetic barrier, such that the overall barrier for the protonation of the leaving group is roughly given by the combined free energy costs of forming the initial structure (~17 kcal mol^{-1}, Figure S2) and the hydronium ion (up to ~10 kcal mol^{-1}, assuming bulk-like conditions). The overall barrier would thus be <27 kcal mol^{-1}, which would not entirely rule out the protonation of the leaving group via the O2' oxygen.

E188A Mutation. To study the effect of the Glu188 position in the active site on the mechanism, we performed calculations of a E188A mutant RNase H. The Glu side chain was replaced by an Ala sidechain and a water molecule, which was coordinated to metal ion A. The system was energy minimized, and the nucleophilic attack was driven by harmonic bias potentials applied to reaction coordinate Q_e, without a bias on the proton transfer. As shown in Movie 3, we found that in E188A a proton of the attacking water is transferred via an intermediate water molecule to the *pro*-R_p oxygen of the downstream phosphate, as in the wild type enzyme.

Complete author list for reference 24:

Shao, Y.; Molnar, L. F.; Jung, Y.; Kussmann, J.; Ochsenfeld, C.; Brown, S. T.; Gilbert, A. T. B.; Slipchenko, L. V.; Levchenko, S. V.; O'Neill, D. P.; Jr, R. A. D.; Lochan, R. C.; Wang, T.; Beran, G. J. O.; Besley, N. A.; Herbert, J. M.; Lin, C. Y.; Voorhis, T. V.; Chien, S. H.; Sodt, A.; Steele, R. P.; Rassolov, V. A.; Maslen, P. E.; Korambath, P. P.; Adamson, R. D.; Austin, B.; Baker, J.; Byrd, E. F. C.; Dachsel, H.; Doerksen, R. J.; Dreuw, A.; Dunietz, B. D.; Dutoi, A. D.; Furlani, T. R.; Gwaltney, S. R.; Heyden, A.; Hirata, S.; Hsu, C.-P.; Kedziora, G.; Khalliulin, R. Z.; Klunzinger, P.; Lee, A. M.; Lee, M. S.; Liang, W.; Lotan, I.; Nair, N.; Peters, B.; Proynov, E. I.; Pieniazek, P. A.; Rhee, Y. M.; Ritchie, J.; Rosta, E.; Sherrill, C. D.; Simmonett, A. C.; Subotnik, J. E.; Woodcock, H. L.; Zhang, W.; Bell, A. T.; Chakraborty, A. K.

References

(1) Nowotny, M.; Gaidamakov, S. A.; Crouch, R. J.; Yang, W. *Cell* **2005**, *121*, 1005.
(2) Mandel, A. M.; Akke, M.; Palmer, A. G. *J. Mol. Biol.* **1995**, *246*, 144.
(3) Nowotny, M.; Yang, W. *EMBO J.* **2006**, *25*, 1924.
(4) De Vivo, M.; Dal Peraro, M.; Klein, M. L. *J. Am. Chem. Soc.* **2008**, *130*, 10955.

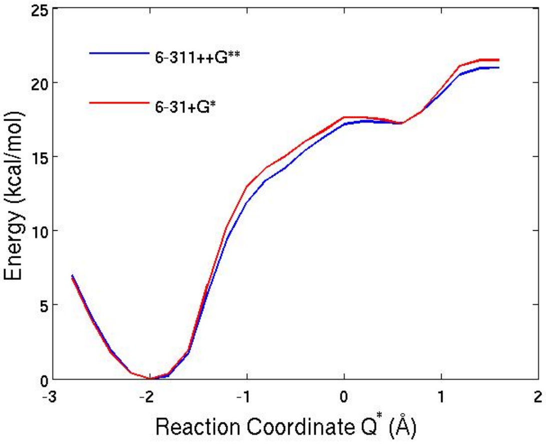

Figure S1. Basis set effects on the calculated energies. Structures were obtained by energy minimization using the 6-31+G* basis set for the first reaction step with Asp132 unprotonated. The figure compares the energies of these structures obtained with the 6-31+G* basis set (red) and the 6-311++G** basis set (blue) as a function of the reaction coordinate Q*=ET+(PT1a+PT1b)/2.

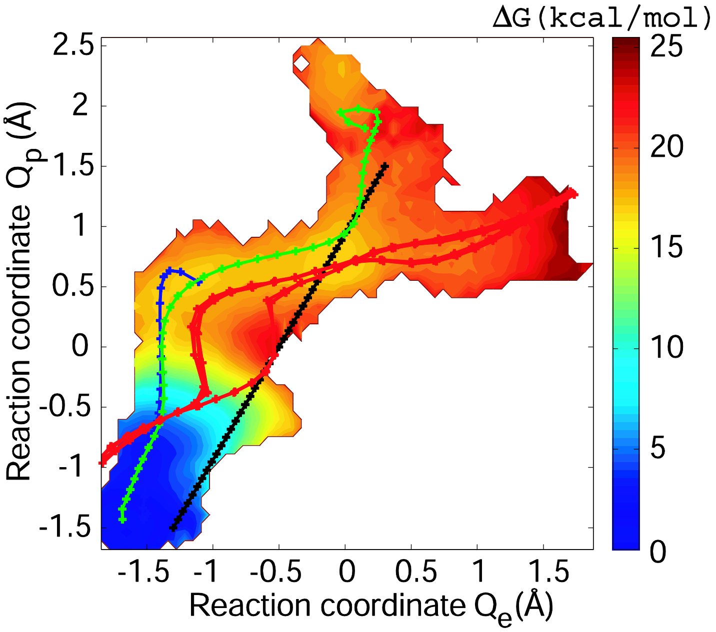

Figure S2. 2D-free energy surface and reaction pathways corresponding to the first step of the RNase H reaction with unprotonated Asp132 obtained by projection onto coordinates Q_e=ET and Q_p=0.5*(PT1a+PT1b). The black curve shows the initial string; the blue and green curves show the converged strings using shorter and longer strings, respectively, the red curve shows the minimization pathway on top of the free energy surface.

```
Ec    1 MLKQVEIFTDGSCLGNPGPGGYGAILRYRGREKTFSAGY---TRTTNNRMELMAAIVALE

Hs  136 MGDFVVVYTDGCCSSNGRRRPRAGIGVYWGPGHPLNVGIRLPGRQTNQRAEIHAACKAIE

HIV 434 IVGAETFYVDGAANRETKLG-KAGYVTNKGRQKVVPLTD-----TTNQKTELQAIYLALQ

Bh   62 EIIWESLSVDVGSQGNPGIVEYKGVDTKTGEVLFEREPIP---IGTNNMGEFLAIVHGLR


Ec   58 ALKEH--CEVILSTDSQYVRQGITQWIHNWKKRGWKTADKKPVKNVDLWQRLDAALGQHQ

Hs  196 QAKTQNINKLVLYTDSMFTINGITNWVQGWKKNGWKTSAGKEVINKEDFVALERLTQGMD

HIV 488 DSGLE----VNIVTDSQYALGIIQAQPD---------ESESELVN----QIIEQLIKKEK

Bh  119 YLKERN-SRKPIYSDSQTAIK----WVKDKKAKSTLVRNEETALIWKLVDEAEEWLNTHT


Ec  116 IKWEWVK------GHAGHPENERCDELARAAAMNPTLEDTGYQVEV 155

Hs  256 IQWMHVP------GHSGFIGNEEADRLAREGAKQS--ED------- 286

HIV 531 VYLAWVP------AHKGIGGNEQVDKLVSA---------------- 554

Bh  174 YETPILKWQTDKWGE------IKADYGRK----------------- 196
```

Figure S3. Sequence alignment of catalytic domains of RNases H: Ec, *E. coli*; Hs, human; HIV, HIV RT; Bh, *Bc. halodurans* species. Conserved catalytic carboxylate residues are highlighted in red. A conserved serine residue is highlighted in yellow. The conserved His (or Glu in case of *Bh*) is shown in green.

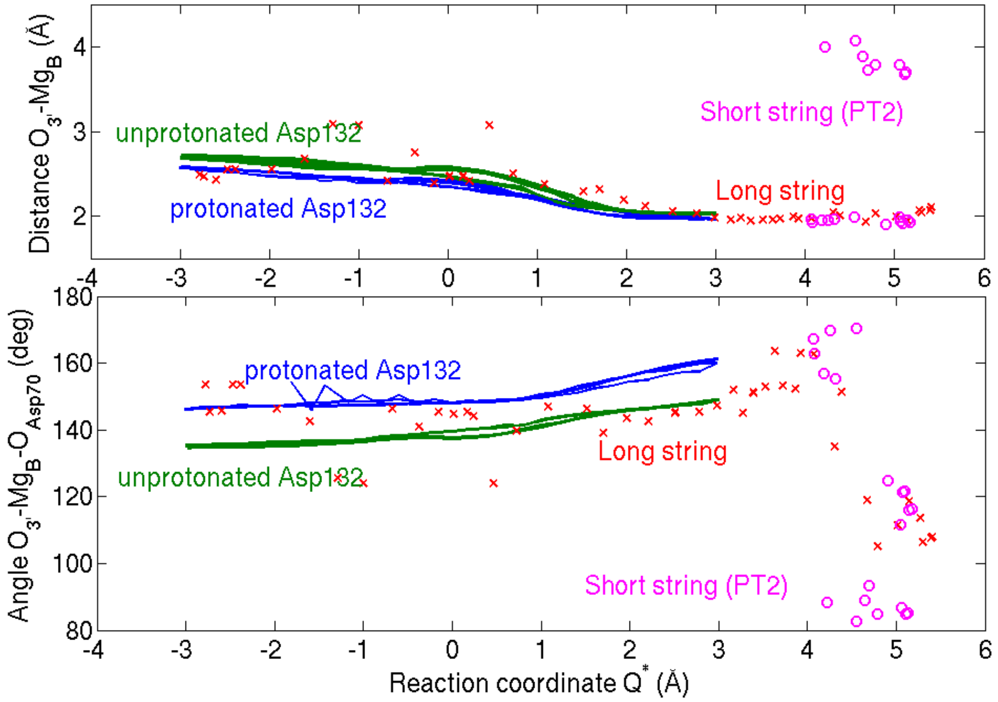

Figure S4. Changes in the coordination of the Mg^{2+} ion B. (Top) The distance of the leaving group and the coordinating Mg2+ ion is shown as a function of the reaction coordinate Q*=ET+0.5*(PT1a+PT1b). (Bottom) The axial angle between the leaving group oxygen, the pentacoordinated Mg2+ ion, and the bridging Asp71 is plotted as a function of the reaction coordinate. Results are shown for the long string (red), connecting reactant (RS) and product states (PS), and for the short string (purple) between intermediate (IS) and product states. Also shown are the results of repeated minimizations with protonated (blue) and unprotonated Asp132 (green).